The α-arrestin ARRDC3 mediates ALIX ubiquitination and G protein–coupled receptor lysosomal sorting

Michael R. Dores, Huilan Lin, Neil J. Grimsey, Francisco Mendez, and JoAnn Trejo
Department of Pharmacology, School of Medicine, University of California, San Diego, La Jolla, CA 92093

ABSTRACT **The sorting of G protein–coupled receptors (GPCRs) to lysosomes is critical for proper signaling and cellular responses. We previously showed that the adaptor protein ALIX regulates lysosomal degradation of protease-activated receptor-1 (PAR1), a GPCR for thrombin, independent of ubiquitin-binding ESCRTs and receptor ubiquitination. However, the mechanisms that regulate ALIX function during PAR1 lysosomal sorting are not known. Here we show that the mammalian α-arrestin arrestin domain–containing protein-3 (ARRDC3) regulates ALIX function in GPCR sorting via ubiquitination. ARRDC3 colocalizes with ALIX and is required for PAR1 sorting at late endosomes and degradation. Depletion of ARRDC3 by small interfering RNA disrupts ALIX interaction with activated PAR1 and the CHMP4B ESCRT-III subunit, suggesting that ARRDC3 regulates ALIX activity. We found that ARRDC3 is required for ALIX ubiquitination induced by activation of PAR1. A screen of nine mammalian NEDD4-family E3 ubiquitin ligases revealed a critical role for WWP2. WWP2 interacts with ARRDC3 and not ALIX. Depletion of WWP2 inhibited ALIX ubiquitination and blocked ALIX interaction with activated PAR1 and CHMP4B. These findings demonstrate a new role for the α-arrestin ARRDC3 and the E3 ubiquitin ligase WWP2 in regulation of ALIX ubiquitination and lysosomal sorting of GPCRs.**

Monitoring Editor
Jean E. Gruenberg
University of Geneva

Received: May 15, 2015
Revised: Oct 15, 2015
Accepted: Oct 16, 2015

INTRODUCTION

G protein–coupled receptors (GPCRs) make up the largest family of mammalian signaling receptors and major pharmaceutical targets for the treatment of many human diseases, including cancer, cardiovascular disease, and chronic inflammatory disorders (Mason *et al.*, 2012; O'Hayre *et al.*, 2014). Lysosomal sorting and degradation of GPCRs is critical for proper control of signaling and cellular responses (Marchese *et al.*, 2008; Marchese and Trejo, 2012). Multiple pathways exist to sort mammalian GPCRs to lysosomes for degradation. The best-characterized pathway is an evolutionarily conserved process that requires receptor ubiquitination and the endosomal sorting complexes required for transport (ESCRT) machinery. Ubiquitin-binding proteins within the ESCRT-0 and ESCRT-I complexes interact with GPCRs posttranslationally modified with ubiquitin to facilitate the sorting of receptors at the early endosome. GPCRs are then packaged into intraluminal vesicles by the ESCRT-II and III complexes, forming multivesicular endosomes (MVEs) that then fuse with lysosomes. We previously identified an alternative pathway for sorting GPCRs into the MVE that is dependent on the adaptor protein ALG-interacting protein X (ALIX) and does not require direct GPCR ubiquitination and ESCRT-0 and -I complexes (Gullapalli *et al.*, 2006; Wolfe *et al.*, 2007; Dores *et al.*, 2012a). ALIX regulates the degradation of protease-activated receptor-1 (PAR1), a GPCR for thrombin (Soh and Trejo, 2011), by coupling PAR1 to the ESCRT-III complex subunit CHMP4 (Dores *et al.*, 2012a). However, the mechanisms that regulate ALIX-dependent GPCR sorting at multivesicular endosomes remain poorly understood.

ALIX has been shown to interact with the mammalian α-arrestins during viral budding at the plasma membrane (Rauch and Martin-Serrano, 2011). The mammalian α-arrestin family includes five

This article was published online ahead of print in MBoC in Press (http://www.molbiolcell.org/cgi/doi/10.1091/mbc.E15-05-0284) on October 21, 2015.

Address correspondence to: JoAnn Trejo (joanntrejo@ucsd.edu).

Abbreviations used: AIP4, atrophin1-interacting protein 4; ALIX, ALG-interacting protein X; ARRDC, arrestin domain–containing protein; β2-AR, β2-adrenergic receptor; BRET, bioluminescence resonance energy transfer; EEA1, early endosome antigen 1; EGFR, epidermal growth factor receptor; ESCRT, endosomal complexes required for transport; GPCR, G protein–coupled receptor; HRS, hepatocyte growth factor–regulated tyrosine kinase substrate; MVE, multivesicular endosome; NEDD4, neural precursor cell–expressed, developmentally down-regulated protein 4; PAR1, protease-activated receptor-1; Rluc, *Renilla reniformis* luciferase; SMURF, Smad ubiquitin regulatory factor 1; WWP2, WW domain–containing E3 ubiquitin protein ligase 2; YFP, yellow fluorescent protein.

arrestin domain–containing proteins (ARRDCs) and thioredoxin-interacting protein (TXNIP) that share similar domain homology with the mammalian β-arrestins (Alvarez, 2008). ALIX binds to the C-terminal region of TXNIP and ARRDCs 1–4 (Rauch and Martin-Serrano, 2011). These α-arrestins also harbor PPXY motifs within the C-terminal region that are required for interaction with neural precursor cell–expressed, developmentally down-regulated protein 4 (NEDD4)–family E3 ubiquitin ligases (Nabhan *et al.*, 2010; Rauch and Martin-Serrano, 2011; Shea *et al.*, 2012). ARRDC1 forms a complex with NEDD4.1 and ALIX at the plasma membrane, facilitating the assembly of the ALIX-dependent ESCRT complex during the late stages of viral budding (Rauch and Martin-Serrano, 2011). In addition, NEDD4.1 mediates ubiquitination of ALIX during viral budding, suggesting that ALIX function may be regulated by ubiquitination (Sette *et al.*, 2010). ALIX harbors a ubiquitin-binding domain within the central V-domain (Keren-Kaplan *et al.*, 2013; Pashkova *et al.*, 2013), and ubiquitination of ALIX may regulate its dimerization. Of interest, ALIX ubiquitin-binding is required for dimerization in vitro (Keren-Kaplan *et al.*, 2013). Dimerization of ALIX facilitates the recruitment of the ESCRT-III complex (Pires *et al.*, 2009), and dimerized ALIX localizes to internal endosomal punctae (Bissig *et al.*, 2013). These findings suggest that ARRDCs may mediate E3 ligase recruitment to ALIX and may regulate ALIX ubiquitination and function at endosomes.

ARRDCs may also regulate GPCR sorting at endosomes. The β2-adrenergic receptor (β2-AR) is ubiquitinated after agonist stimulation, and receptor ubiquitination appears to facilitate lysosomal degradation (Shenoy *et al.*, 2008). ARRDC1 and ARRDC3 colocalize and associate with agonist-activated β2-AR at endosomes (Nabhan *et al.*, 2010; Han *et al.*, 2012; Shea *et al.*, 2012). Agonist-stimulated β2-AR ubiquitination was inhibited by small interfering RNA (siRNA)–mediated depletion of ARRDC3 and overexpression of an ARRDC3 mutant lacking functional PPXY motifs (Nabhan *et al.*, 2010; Shea *et al.*, 2012). These data suggest that ARRDC3 recruits NEDD4.1 to ubiquitinate β2-AR. However, further studies demonstrated that β-arrestins function as the primary adaptors to recruit NEDD4.1 to facilitate ubiquitination of β2-AR after agonist stimulation (Han *et al.*, 2012), whereas ARRDC3 is recruited secondarily to the β2-AR/NEDD4.1 complex at endosomes and facilitates trafficking to a subpopulation of early endosomes (Han *et al.*, 2012). Of interest, ARRDC3 binds to β-arrestins and hepatocyte growth factor–regulated tyrosine kinase substrate (HRS), a component of the ESCRT-0 complex that binds ubiquitinated receptors at early endosomes (Shea *et al.*, 2012). Thus ARRDC3 may regulate the stability and recruitment of the protein complexes that mediate β2-AR sorting at endosomes. However, further work is required to identify the exact function of α-arrestins in the endosomal/lysosomal sorting of GPCRs that require ubiquitination for degradation like the β2-AR.

In contrast to the β2-AR, the role of ARRDCs in the regulation of ALIX-dependent GPCR degradation has not been examined. Here we report that the α-arrestin ARRDC3 mediates degradation of activated PAR1 by regulating receptor sorting into the lumen of multivesicular endosomes. PAR1, ARRDC3, and ALIX colocalize on endosomes, and ARRDC3 is required for ALIX interaction with PAR1 and the ESCRT-III subunit CHMP4B. Moreover, activation of PAR1 increases ALIX ubiquitination that is dependent on ARRDC3 and WW domain–containing E3 ubiquitin protein ligase 2 (WWP2). In addition, the depletion of WWP2 not only blocks ALIX ubiquitination, but it also inhibits the capacity of ALIX to bind PAR1 and CHMP4B, which is essential for PAR1 degradation. These findings demonstrate that ARRDC3 regulates ALIX during GPCR lysosomal sorting and suggest that WWP2-dependent ALIX ubiquitination is required for the packaging of PAR1 into intraluminal vesicles of multivesicular endosomes.

RESULTS

PAR1 interacts with ARRDC3

The mechanisms that regulate ALIX function in GPCR lysosomal sorting are not known. We hypothesize that ALIX binding partners such as ARRDC3 may serve an important function in PAR1 endosomal/lysosomal sorting. To characterize the function of ARRDC3 in PAR1 trafficking, we used bioluminescence resonance energy transfer (BRET) to test whether ARRDC3 interacts with PAR1 in living cells. COS7 cells coexpressing a constant amount of ARRDC3 fused to *Renilla reniformis* luciferase (Rluc) and increasing amounts of PAR1 fused to yellow fluorescent protein (YFP) exhibited changes in net BRET. The net BRET signal increased and saturated as the ratio of PAR1 to ARRDC3 was increased, indicating that ARRDC3 and PAR1 specifically interact (Figure 1A). In contrast, cells expressing ARRDC3 Rluc and the related thrombin receptor PAR4 did not exhibit significant changes in net BRET, and the BRET signal failed to saturate, indicating a nonspecific interaction (Figure 1A). These data suggest that ARRDC3 specifically interacts with PAR1 in comparison to other PARs. A fixed ratio of PAR1-YFP to ARRDC3-Rluc was then used to examine whether stimulation of PAR1 with thrombin affected the interaction. Under control conditions, PAR1/ARRDC3 exhibited a substantial BRET signal compared with PAR4/ARRDC3, which was used as a negative control (Figure 1B). Incubation with thrombin did not significantly alter the BRET signal between ARRDC3 and PAR1 or PAR4 (Figure 1B). These findings suggest that ARRDC3 associates with PAR1 basally and that activation of PAR1 does not appear to enhance or disrupt PAR1 and ARRDC3 interaction.

PAR1 resides primarily at the plasma membrane and, after activation, is rapidly internalized and trafficked to early and then late endosomes/lysosomes before degradation (Dores *et al.*, 2012a). Because PAR1 and ARRDC3 remain associated after agonist stimulation (Figure 1B), we examined whether activated PAR1-ARRDC3 colocalizes with ALIX on endosomes, using immunofluorescence confocal microscopy. HeLa cells expressing FLAG-PAR1 were cotransfected with hemagglutinin (HA)-ARRDC3 and ALIX fused to split-YFP. ALIX primarily localizes to the cytoplasm and associates with membranes upon dimerization (Pires *et al.*, 2009; Bissig *et al.*, 2013). Dimerized ALIX can be visualized using split-YFP in which either the N- or C-domain of YFP protein is fused to ALIX lacking its C-terminal proline-rich domain (Bissig *et al.*, 2013). On dimerization, the YFP N- and C-domains interact and fluoresce (Pires *et al.*, 2009; Bissig *et al.*, 2013). The surface cohort of PAR1 was labeled with anti-FLAG antibody at 4°C. In the absence of agonist, ARRDC3 and PAR1 appear to partially colocalize at the plasma membrane, as assessed by confocal microscopy (Figure 1C) and verified by Pearson's *r*, $r = 0.55$. In unstimulated cells, ARRDC3 also colocalizes with ALIX in early and late endosomes (Supplemental Figure S1, A and B). In contrast, surface-labeled PAR1 and ALIX are not colocalized in untreated cells (Figure 1C). We next examined whether activation of PAR1 affected colocalization with ALIX and ARRDC3, using the agonist peptide SFLLRN, since thrombin cleaves off the N-terminal FLAG epitope of PAR1 (Vu *et al.*, 1991). After 20 min of agonist stimulation, PAR1 sorted to ARRDC3- and ALIX-positive internal punctae (Figure 1C). In addition, the extent of PAR1 colocalization with ARRDC3 and ALIX was increased, as reflected by $r = 0.78$ and 0.67, respectively. Of interest, agonist stimulation did not significantly change the extent of ARRDC3 colocalization with ALIX in early and late endosomes (Supplemental Figure S1C), suggesting that membrane trafficking of PAR1 does not significantly alter the

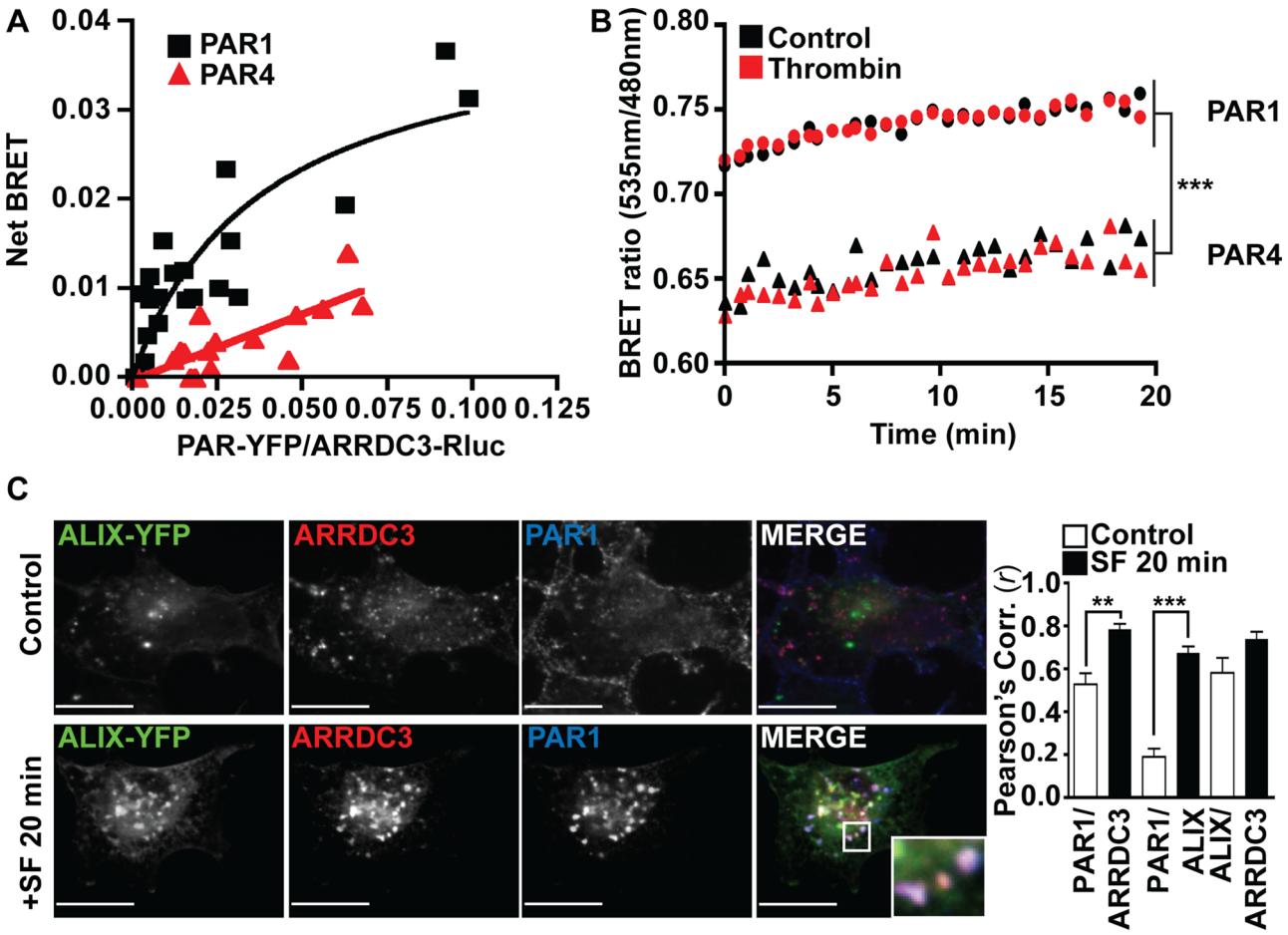

FIGURE 1: ARRDC3 interacts and colocalizes with PAR1. (A) COS7 cells were transfected with ARRDC3-Rluc and an increasing amount of PAR1-YFP or PAR4-YFP. Net BRET was calculated from wells and plotted against the ratio of YFP to Rluc signal. (B) COS7 cells expressing ARRDC3-Rluc and PAR1-YFP or PAR4-YFP were stimulated with 10 nM thrombin or treated with buffer, and the BRET ratio was calculated. Results are representative of three independent experiments. (C) HeLa cells stably expressing FLAG-PAR1 (blue) were transfected with ALIX fused to the N-terminal domain of YFP (YFPn) or C-terminal domain of YFP (YFPc) together with HA-ARRDC3 (red). Cells were stimulated with 100 μM SFLLRN and then fixed, permeabilized, and processed for immunofluorescence microscopy. Scale bars, 10 μM. The colocalization between PAR1, ARRDC3, and ALIX after agonist treatment was quantified by calculating Pearson's *r* of unstimulated and stimulated cells. The data represent the mean ± SD ($n = 6$) and were compared using Student's *t* test (**$p < 0.01$; ***$p < 0.001$).

distribution of ARRDC3 at endosomes. These data demonstrate that activated PAR1 internalizes from the cell surface and colocalizes with both ARRDC3 and dimerized ALIX on endosomes.

ARRDC3 is required for PAR1 degradation

Next we assessed whether ARRDC3 is required for the lysosomal degradation of PAR1. Transfection of HeLa cells expressing PAR1 with ARRDC3-specific siRNAs caused a significant reduction in the expression of endogenous ARRDC3 compared with cells transfected with nonspecific siRNAs (Supplemental Figure S2A). In nonspecific siRNA control–transfected cells, agonist caused a significant ~55% loss of PAR1 protein (Figure 2A, lanes 1 and 2). In contrast, the extent of PAR1 degradation was markedly reduced in cells depleted of endogenous ARRDC3. Only ~15% of PAR1 was degraded after 60 min of agonist incubation (Figure 2A, lanes 5 and 6). As expected, cells transfected with ALIX siRNAs also blocked agonist-driven PAR1 degradation to a similar extent (Figure 2A, lanes 3–6; Dores *et al.*, 2012a). To confirm that ARRDC3 is specifically required for PAR1 degradation, we expressed an siRNA-resistant mutant of ARRDC3 in cells depleted of endogenous ARRDC3 (Supplemental Figure S2B). Activated PAR1 was degraded, reflected by ~50% loss in receptor protein, in cells transfected with nonspecific siRNA and plasmid control (pcDNA) vector (Figure 2B, lanes 1 and 2). However, in cells transfected with ARRDC3 siRNA and pcDNA vector, only ~15% of activated PAR1 is degraded (Figure 2B, lanes 3 and 4). Of importance, agonist-stimulated PAR1 degradation was restored to control levels in cells transfected with ARRDC3 siRNA and siRNA-resistant ARRDC3 (Figure 2B, lanes 5 and 6). These results indicate that ARRDC3 expression is both necessary and sufficient for agonist-promoted PAR1 degradation.

Similar to other GPCRs, PAR1 is ubiquitinated (Wolfe *et al.*, 2007; Chen *et al.*, 2011). However, ubiquitination of PAR1 is not required for lysosomal degradation (Wolfe *et al.*, 2007). In addition, a ubiquitin-deficient PAR1 "0K" mutant lacking all intracellular lysine (K) residues is sorted into intraluminal vesicles of multivesicular endosomes and requires ALIX for degradation (Dores *et al.*, 2012a). To test whether ubiquitin-independent PAR1 degradation also requires ARRDC3, we transfected HeLa cells expressing the PAR1 0K mutant

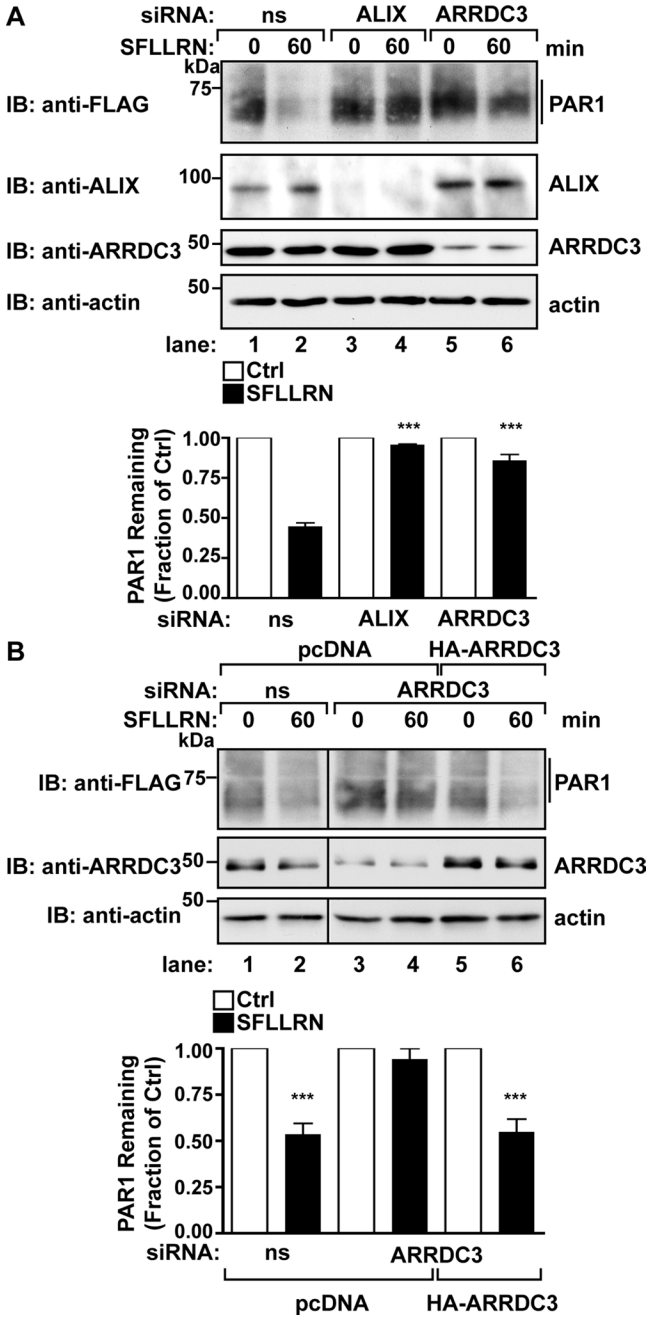

FIGURE 2: ARRDC3 is required for PAR1 degradation. (A) FLAG-PAR1–expressing HeLa cells were transfected with nonspecific (ns) or ALIX- or ARRDC3-specific siRNAs and then stimulated with 100 μM SFLLRN for 60 min. Cell lysates were collected, and the extent of PAR1 degradation was quantified by densitometry. The data represent the mean ± SD ($n = 3$) and were compared using two-way ANOVA (***$p < 0.001$). (B) PAR1-expressing HeLa cells were cotransfected with nonspecific (ns) or ARRDC3-specific siRNAs and either pcDNA vector or siRNA-resistant HA-ARRDC3 and then stimulated for 60 min with 100 μM SFLLRN. The amount of PAR1 remaining was quantified by densitometry. The data represent the mean ± SD ($n = 3$) and were analyzed by two-way ANOVA (***$p < 0.001$, $n = 3$).

with nonspecific or ARRDC3-siRNAs before stimulation with agonist. Cells lacking ARRDC3 expression showed significantly less degradation of PAR1 after agonist incubation than nonspecific siRNA–transfected control cells (Figure 3A). These findings suggest that ARRDC3 regulates ubiquitin-independent lysosomal sorting of receptors. We next examined whether ARRDC3 is required for the lysosomal sorting of ubiquitinated receptors that traffic through the classic ESCRT pathway. The loss of ARRDC3 failed to affect agonist-promoted degradation of the epidermal growth factor receptor (EGFR; Figure 3B), a receptor tyrosine kinase that sorts through a ubiquitin and ESCRT pathway before lysosomal degradation (Duan *et al.*, 2003). In addition, ARRDC3 depletion did not inhibit agonist-induced degradation of PAR2 (Figure 3C), a protease-activated GPCR that requires receptor ubiquitination and ESCRT-0 complexes for lysosomal degradation (Hasdemir *et al.*, 2009). The extent of siRNA-mediated ARRDC3 depletion was comparable under all conditions (Supplemental Figure S3). These results indicate that ARRDC3 is required for ubiquitin-independent lysosomal degradation of PAR1 and suggest that ARRDC3 is not required for the degradation of ubiquitinated receptors that traffic through the canonical ESCRT pathway.

ARRDC3 mediates PAR1 sorting into late/multivesicular endosomes

ARRDC3 colocalizes with PAR1 at the plasma membrane and at endosomes (Figure 1C) and is required for PAR1 degradation (Figure 2). However, it is unclear how ARRDC3 mediates PAR1 endocytic sorting. We first tested whether ARRDC3 depletion inhibits PAR1 internalization, using cell-surface enzyme-linked immunosorbent assay (ELISA). HeLa cells expressing FLAG-PAR1 were surface labeled with anti-FLAG antibody and then stimulated with agonist to induce internalization. Cells were then fixed, and the amount of anti-FLAG antibody remaining on the cell surface was quantified. Agonist stimulation induced ~50% loss of PAR1 from the cell surface in nonspecific siRNA–transfected cells compared with untreated control cells (Figure 4A). The extent of agonist-induced internalization of PAR1 was similar in cells depleted of either ALIX or ARRDC3 expression (Figure 4A), suggesting that ARRDC3 is not required for activated PAR1 internalization. After internalization, PAR1 is sorted from early endosomes to late endosomes/multivesicular endosomes before degradation (Dores *et al.*, 2012a). Confocal immunofluorescence microscopy was used to examine whether ARRDC3 is required for PAR1 sorting at early endosomes. HeLa cells expressing FLAG-PAR1 were prelabeled with anti-FLAG antibody and then stimulated with agonist for the indicated times. Cells were fixed, permeabilized, and immunostained for the early endosomal antigen 1 (EEA1), a membrane-associated marker for the early endosome. In cells treated with either nonspecific or ARRDC3 siRNA, PAR1 exhibited marked internalization and colocalization with EEA1 after 10 min of agonist stimulation, which was verified by Pearson's r (nonspecific siRNA, $r = 0.48$; ARRDC3 siRNA, $r = 0.5$; Figure 4B). After 20 min of agonist stimulation, PAR1 appeared to sort away from EEA1-positive early endosomes in both control and ARRDC3-depleted cells, as demonstrated by a significant reduction to $r = 0.2$ (Figure 4B). These findings indicate that ARRDC3 is not required for PAR1 sorting at the early endosome.

Next we examined whether ARRDC3 is required for PAR1 sorting into the lumen of multivesicular endosomes. To visualize PAR1 incorporation into the lumen of late endosomes, we transfected FLAG-PAR1–expressing cells with a green fluorescent protein (GFP)–tagged, constitutively active Rab Q79L mutant. Expression of Rab5 Q79L causes enlargement of early/late endosomes (Stenmark *et al.*, 1994), a strategy that has been used to interrogate the factors that regulate GPCR sorting into multivesicular endosomes (O'Keeffe *et al.*, 2008; Henry *et al.*, 2011; Dores *et al.*, 2012b). Cells were then transfected with either nonspecific or ARRDC3 siRNAs. After

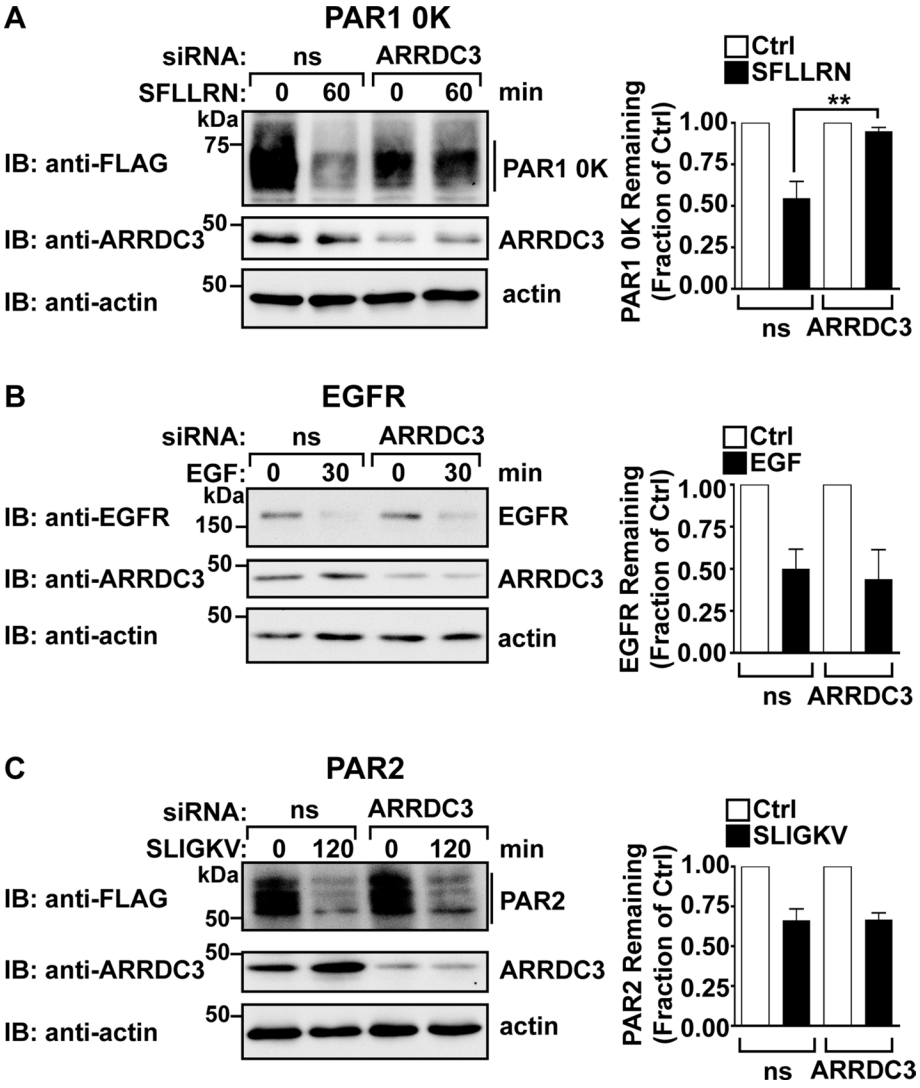

FIGURE 3: ARRDC3 is required for the ubiquitin-independent degradation of PAR1. (A) HeLa cells expressing the FLAG-PAR1 0K mutant were transfected with nonspecific (ns) or ARRDC3 siRNAs and then stimulated for 60 min with 100 μM SFLLRN. Cell lysates were analyzed by immunoblot. The amount of PAR1 0K remaining was quantified by densitometry. The data represent the mean ± SD ($n = 3$) and were compared by two-way ANOVA (**$p < 0.01$). (B) HeLa cells were transfected with nonspecific (ns) or ARRDC3-specific siRNAs and then treated with 10 nM EGF for 30 min. The amount of activated EGFR remaining was quantified, and the data represent the mean ± SD ($n = 3$). (C) HeLa cells expressing FLAG-PAR2 were transfected with nonspecific (ns) or ARRDC3 siRNAs and then stimulated with 100 μM SLIGKV for 120 min. The amount of activated PAR2 remaining was quantified, and the data represent mean ± SD ($n = 3$).

transfections, cells were treated with 2 mM leupeptin to inhibit lysosomal degradation, incubated with anti-FLAG antibody at 4°C to label the PAR1 surface cohort, and stimulated with agonist. In nonspecific siRNA–treated cells, PAR1 accumulation in the lumen of Rab5-positive endosomes was clearly evident after 60 min of stimulation with agonist and was quantified by line-scan analysis (Figure 4C), consistent with previous studies (Dores *et al.*, 2012b). In contrast, activated PAR1 appears to localize at the limiting membrane of Rab5-positive endosomes and be excluded from the lumen of the endosomes in cells depleted of endogenous ARRDC3 (Figure 4C). Taken together, these findings suggest that ARRDC3 regulates PAR1 sorting at late/multivesicular endosomes rather than early in the endocytic pathway.

Depletion of ARRDC3 disrupts ALIX binding to PAR1 and the ESCRT-III complex

The degradation of activated PAR1 requires binding to ALIX, which facilitates interaction between PAR1 and the ESCRT-III complex (Dores *et al.*, 2012a). We next examined whether ARRDC3 is required for PAR1 interaction with ALIX. HeLa cells expressing FLAG-PAR1 were transfected with nonspecific or ARRDC3 siRNAs and then stimulated with agonist. Cells were lysed and immunoprecipitated with anti-FLAG antibody, and the coprecipitation of ALIX was assessed by immunoblot. In nonspecific siRNA–transfected cells, endogenous ALIX coimmunoprecipitated with activated PAR1 at 10 min (Figure 5A, lanes 2–4), whereas ARRDC3 depletion significantly reduced ALIX interaction with activated PAR1 (Supplemental Figure S4A and Figure 5A, lanes 5–7). These results suggest that the loss of ARRDC3 disrupts the capacity of ALIX to bind to activated PAR1. We next tested whether depletion of ARRDC3 inhibits ALIX binding to the ESCRT-III subunit CHMP4B after PAR1 activation. ALIX binds to CHMP4B via its N-terminal Bro1 domain (McCullough *et al.*, 2008), and ALIX is required for CHMP4B interaction with activated PAR1 (Dores *et al.*, 2012a). PAR1-expressing HeLa cells were transfected with HA-CHMP4B and either nonspecific or ARRDC3 siRNAs and then incubated with agonist. Cell lysates were immunoprecipitated with anti-HA (CHMP4B) antibody, and the coprecipitation of ALIX was assessed by immunoblot. In cells transfected with nonspecific siRNA, activation of PAR1 increased endogenous ALIX coimmunoprecipitation with CHMP4B (Figure 5B, lanes 2 and 3). In contrast, ARRDC3 depletion caused a slight increase in basal interaction between ALIX and CHMP4B that was not statistically significant when compared with nonspecific samples (Supplemental Figure S4B and Figure 5B, lane 5). However, stimulation of PAR1 did not induce ALIX interaction with CHMP4B in agonist-stimulated cells lacking ARRDC3 (Figure 5B, lane 6). These findings suggest that ARRDC3 regulates ALIX at the late endosome by facilitating ALIX interaction with both PAR1 and the ESCRT-III complex.

ARRDC3 mediates ALIX ubiquitination

ALIX becomes ubiquitinated during viral budding (Sette *et al.*, 2010), suggesting that ubiquitination may be important for ALIX function. However, ALIX ubiquitination in response to GPCR activation has not been previously examined. PAR1-expressing HeLa cells were transfected with HA-ALIX and incubated with agonist. ALIX was immunoprecipitated with anti-HA antibody, and ubiquitination was assessed by immunoblot using an anti-ubiquitin antibody. ALIX appears to be ubiquitinated under basal conditions (Figure 6A, lane

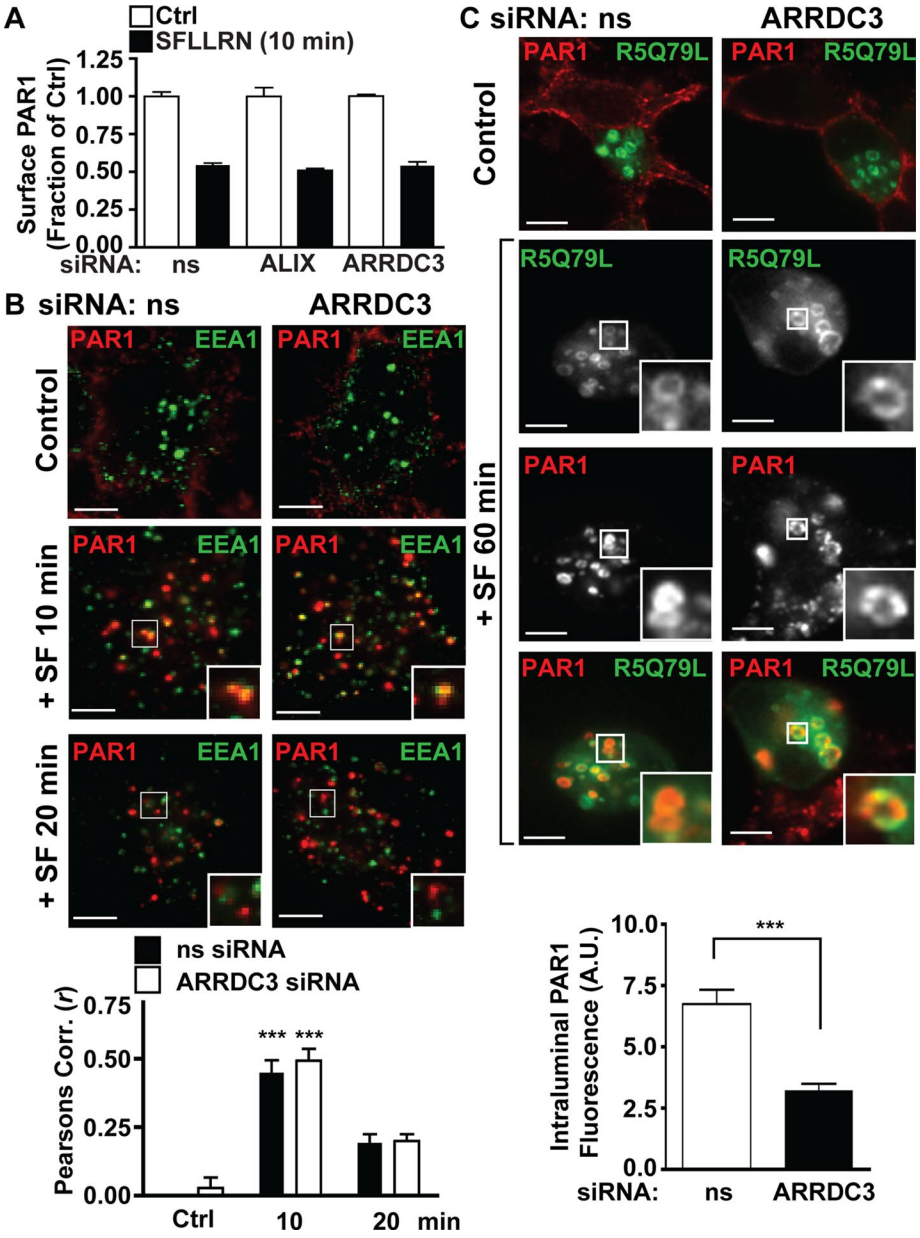

FIGURE 4: ARRDC3 is required for PAR1 sorting at late endosomes. (A) HeLa cells expressing FLAG-PAR1 were transfected with nonspecific (ns), ALIX, or ARRDC3 siRNA and then stimulated with 100 µM SFLLRN. The remaining surface PAR1 was measured by ELISA. The data represent the mean ± SD ($n = 3$). (B) HeLa cells expressing FLAG-PAR1 (red) were transfected with ns or ARRDC3 siRNA. Cells were stimulated with 100 µM SFLLRN and then fixed and stained with anti-EEA1 antibody (green). Insets show magnification of the boxed regions. Scale bars, 10 µm. The data (mean ± SD, $n = 6$) represent Pearson's r calculated for PAR1 and EEA1 and were compared using Student's t test (***$p < 0.001$). (C) ARRDC3 is required for PAR1 sorting into MVEs. FLAG-PAR1 HeLa cells were cotransfected with GFP-Rab5 Q79L and either ns or ARRDC3 siRNA. Cells were treated with leupeptin and then stimulated for 60 min with 100 µM SFLLRN. The data (mean ± SD, $n = 6$) represent the fluorescence intensity of PAR1 inside Rab5-positive endosomes as measured by line scan. The data were compared using Student's t test (***$p < 0.001$).

2), consistent with previous findings (Sette *et al.*, 2010, 2013). However, approximately threefold increase in ALIX ubiquitination was evident after 10 min of agonist stimulation (Figure 6A, lane 3), which returned to basal levels at 20 min (Figure 6A, lane 4). These results suggest that ALIX ubiquitination is a regulated response to GPCR activation. We next tested whether ARRDC3 is required for PAR1-stimulated ALIX ubiquitination. We transfected FLAG-PAR1 HeLa cells with HA-ALIX and either nonspecific or ARRDC3 siRNAs and then treated them with agonist. Cells were lysed and immunoprecipitated with anti-HA antibody, and the ubiquitination of ALIX was determined. In cells treated with nonspecific siRNA, activation of PAR1 induced ALIX ubiquitination (Supplemental Figure S5 and Figure 6B, lanes 2–4); however, cells depleted of ARRDC3 failed to exhibit a significant increase in ALIX ubiquitination after agonist stimulation (Figure 6B, lanes 6–8). These results indicate that ARRDC3 is required for ALIX ubiquitination induced by activation of PAR1.

WWP2 E3 ubiquitin ligase mediates PAR1 degradation

We next sought to define the E3 ubiquitin ligase that mediates ALIX ubiquitination induced by GPCR activation. ARRDC3 contains two PPxY motifs within its C-terminus that bind to the WW domains of NEDD4-family HECT domain–containing E3 ubiquitin ligases, including atrophin1-interacting protein 4 (AIP4), WWP1, WWP2, NEDD4.1, and NEDD4.2 (Nabhan *et al.*, 2010; Rauch and Martin-Serrano, 2011; Han *et al.*, 2012; Shea *et al.*, 2012). An siRNA screen of all nine NEDD4 family members was performed to determine whether any of the NEDD4-family E3 ligases are required for PAR1 degradation, a receptor that does not require direct ubiquitination for lysosomal sorting (Dores *et al.*, 2012a). FLAG-PAR1 HeLa cells were transfected with nonspecific siRNAs, or siRNAs targeting each of the nine E3 ubiquitin ligases of the NEDD4 family. Transfection of siRNAs specific to the Smad ubiquitin regulatory factor 1 (SMURF1), SMURF2, NEDL1, NEDL2, AIP4, or WWP1 E3 ligases reduced expression of the target mRNA but did not significantly inhibit agonist-induced PAR1 degradation (Figure 7, A and D). Similarly, NEDD4.1 and NEDD4.2 expression was reduced in siRNA-transfected cells (Supplemental Figure S6A) but failed to affect activated PAR1 degradation compared with nonspecific siRNA–transfected cells (Figure 7, B and D). In contrast, siRNA-mediated depletion of WWP2 caused a marked inhibition of agonist-driven PAR1 degradation, and only ~15% of receptor was degraded after 60 min of agonist incubation (Figures 7, C and D). PAR1 expression at the cell surface was not affected in WWP2-depleted cells (Supplemental Figure S6B). Although ubiquitination of PAR1 is not required for lysosomal sorting (Dores *et al.*, 2012a), the receptor is ubiquitinated after agonist stimulation (Wolfe *et al.*, 2007; Chen *et al.*, 2011). However, WWP2 depletion failed to affect agonist-induced ubiquitination of PAR1 (Supplemental Figure S6C), suggesting

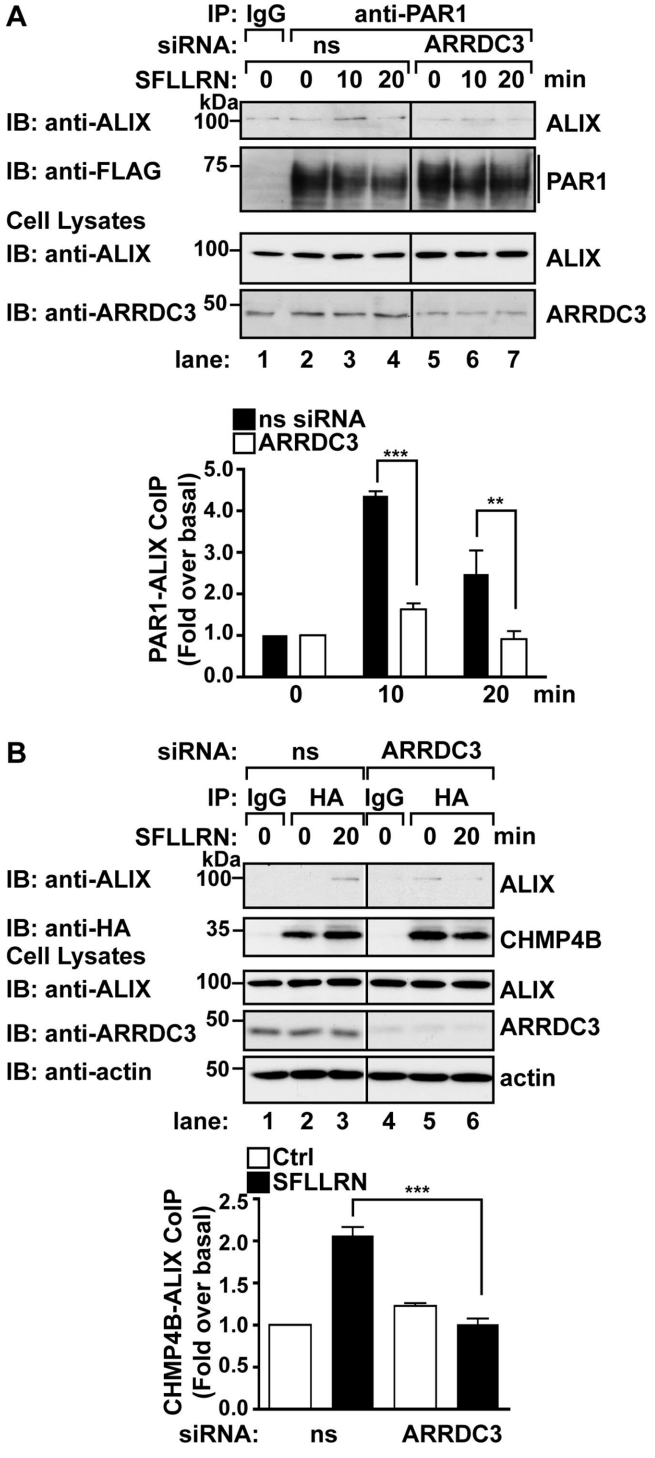

FIGURE 5: ARRDC3 mediates ALIX interaction with PAR1 and the ESCRT-III complex. (A) HeLa cells expressing FLAG-PAR1 were transfected with nonspecific (ns) or ARRDC3 siRNA and then stimulated for the indicated times with 100 μM SFLLRN. FLAG-PAR1 immunoprecipitates were probed with anti-ALIX antibody. ALIX precipitation was quantified by densitometry, and the data (mean ± SD, $n = 3$) were analyzed using two-way ANOVA (***$p < 0.001$; **$p < 0.01$). (B) HeLa cells expressing FLAG-PAR1 were cotransfected with HA-CHMP4B and either ns or ARRDC3 siRNA and then stimulated for the indicated times with 100 μM SFLLRN. HA-CHMP4B immunoprecipitates were probed with anti-ALIX antibody. ALIX precipitation was quantified by densitometry, and the data (mean ± SD, $n = 3$) were analyzed using two-way ANOVA (***$p < 0.001$).

that WWP2 may modulate an important regulator of PAR1 lysosomal sorting rather than the receptor itself. These findings indicate that activated PAR1 lysosomal sorting is regulated by WWP2 E3 ubiquitin ligase through a mechanism that does not appear to affect direct receptor ubiquitination.

WWP2 mediates ALIX ubiquitination

Previous studies proposed that α-arrestins recruit E3 ubiquitin ligases to ALIX during viral budding (Rauch and Martin-Serrano, 2011); however, the NEDD4.1 E3 ligase has been shown to bind to and ubiquitinate ALIX (Sette *et al.*, 2010). Because ARRDC3 is required for ALIX ubiquitination (Figure 6B), we examined whether ARRDC3 is required for ALIX interaction with WWP2. COS7 cells transfected with FLAG-WWP2 and either HA-ARRDC3 or HA-ALIX were lysed and immunoprecipitated with anti-FLAG antibody. Coprecipitation of ARRDC3 with WWP2 was easily detected compared with immunoglobulin G (IgG) control (Figure 8A, lanes 1 and 2), consistent with previous findings (Rauch and Martin-Serrano, 2011; Shea *et al.*, 2012). We observed that expression of ARRDC3 caused a decrease in levels of WWP2 compared with ALIX (Supplemental Figure S7A), suggesting that ARRDC3 interaction with WWP2 might regulate WWP2 turnover. In contrast, WWP2 expression levels were higher when coexpressed with HA-ALIX, and ALIX failed to coprecipitate with FLAG-WWP2 (Figure 8A, lanes 3 and 4). Next we examined whether ectopic expression of ARRDC3 could facilitate WWP2 interaction with ALIX. COS7 cells coexpressing FLAG-WWP2 and either HA-ARRDC3 wild type or HA-ARRDC3 R320Z, a truncation mutant that cannot bind to E3 ligases or ALIX (Rauch and Martin-Serrano, 2011), were immunoprecipitated with anti-FLAG antibody. As previously observed, WWP2 expression was reduced in cells expressing ARRDC3 WT but not the mutant ARRDC3 R320Z (Supplemental Figure S7B), leading to a reduction in immunoprecipitated WWP2 (Supplemental Figure S7C). In contrast, expression of either ARRDC3 WT or ARRDC3 R320Z did not significantly affect endogenous ALIX expression (Supplemental Figure S7B). ALIX coprecipitated with WWP2 in cells expressing ARRDC3 wild type (Figure 8B, lane 3) but not in ARRDC3 R320Z–expressing cells (Figure 8B, lane 4). These results suggest that ARRDC3 mediates the interaction between WWP2 and ALIX and requires its C-terminal binding domain.

WWP2 mediates ALIX ubiquitination and binding to PAR1 and the ESCRT-III complex

Next we assessed whether WWP2 is required for ALIX ubiquitination. We transfected PAR1-expressing HeLa cells with HA-ALIX and stimulated them with agonist. We then analyzed the ubiquitination status of ALIX by immunoblot using an anti-ubiquitin antibody. PAR1 stimulation induced approximately threefold increase in ALIX ubiquitination in cells transfected with nonspecific siRNA (Figure 9A, lanes 1–3). However, depletion of WWP2 resulted in significant attenuation of ALIX ubiquitination (Figure 9A, lanes 4–6). These data indicate that WWP2 is required for ubiquitination of ALIX in response to activation of PAR1. Because WWP2 is required for ALIX ubiquitination, we examined whether WWP2 depletion disrupts ALIX binding to PAR1. We transfected HeLa cells expressing FLAG-PAR1 with nonspecific or ARRDC3 siRNAs and then treated them with agonist. We immunoprecipitated cell lysates with anti-FLAG antibody and assessed coprecipitation of endogenous ALIX by immunoblot. In nonspecific siRNA–transfected cells, ALIX coprecipitated with activated PAR1 (Figure 9B, lane 3), whereas in cells depleted of WWP2, ALIX interaction with PAR1 was markedly reduced (Figure 9B, lanes 5 and 6). These results suggest that WWP2

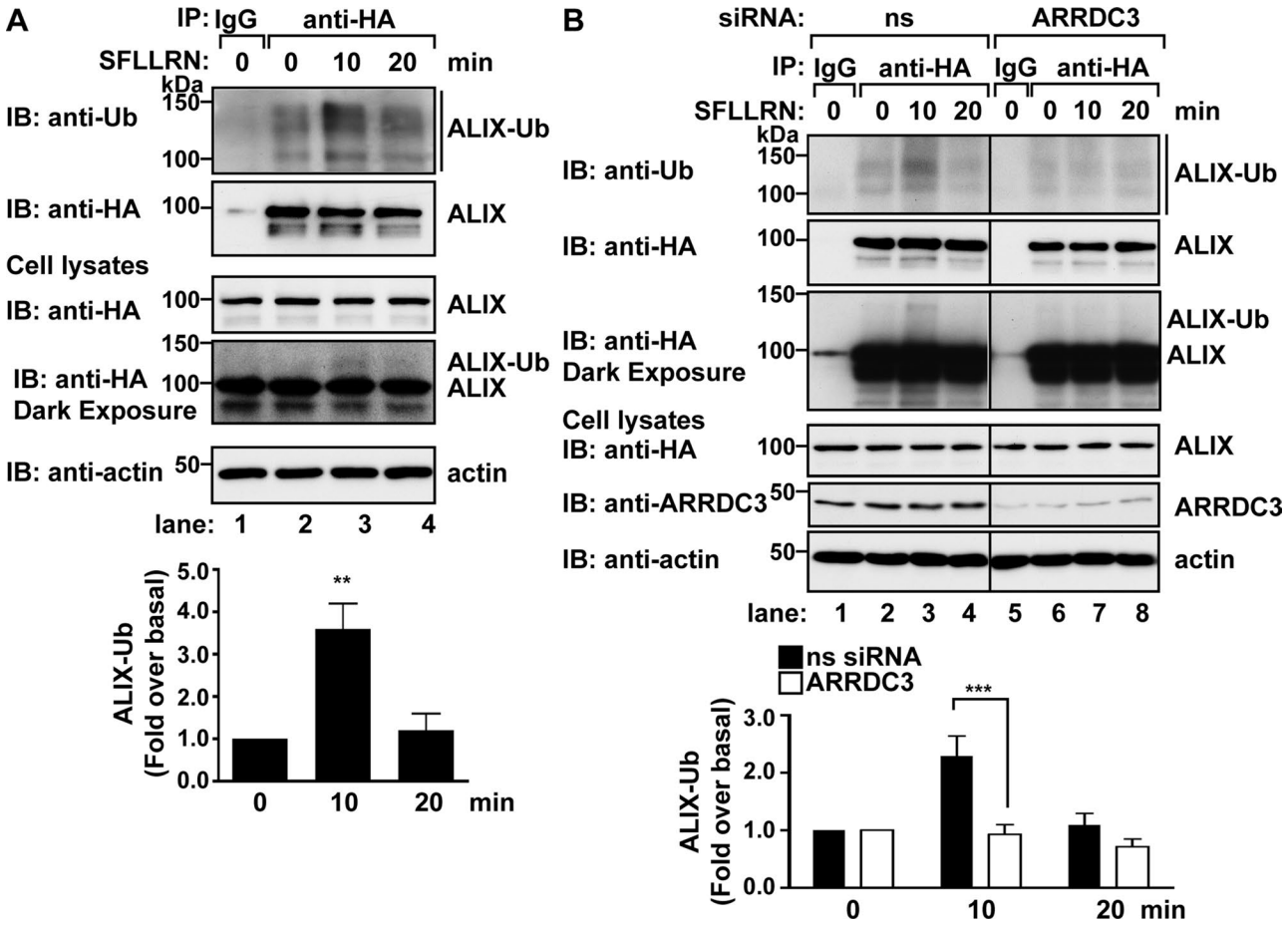

FIGURE 6: ARRDC3 mediates ALIX ubiquitination after PAR1 stimulation. (A) FLAG-PAR1 HeLa cells were transfected with HA-ALIX and then stimulated with 100 μM SFLLRN. Cell lysates were immunoprecipitated with anti-HA antibody and then analyzed by immunoblot with anti-ubiquitin antibodies. ALIX ubiquitination was quantified by densitometry, and the data (mean ± SD, $n = 3$) were analyzed using two-way ANOVA (**$p < 0.01$). (B) FLAG-PAR1 HeLa cells were transfected with HA-ALIX and either nonspecific (ns) or ARRDC3 siRNAs and then stimulated with 100 μM SFLLRN. Cell lysates were immunoprecipitated with anti-HA antibody and then analyzed by immunoblot with anti-ubiquitin antibodies. ALIX ubiquitination was quantified by densitometry, and the data (mean ± SD, $n = 3$) were analyzed using two-way ANOVA (***$p < 0.001$).

mediates ALIX binding to PAR1. We next determined whether WWP2 is required for ALIX interaction with CHMP4B. We transfected HeLa cells expressing FLAG-PAR1 with HA-CHMP4B and either nonspecific or ARRDC3 siRNAs, incubated them with agonist, and lysed them. ALIX coprecipitated with CHMP4B after agonist stimulation in nonspecific siRNA–treated cells (Figure 9C, lane 3). However, ALIX coprecipitation with CHMP4B was substantially reduced in cells deficient in WWP2 expression (Figure 9C, lanes 5 and 6). The extent of ARRDC3 depletion was consistent throughout these experiments (Supplemental Figure S8). These results demonstrate that WWP2 is required for ALIX binding to CHMP4B after activation of PAR1. Taken together, these data indicate that ARRDC3 coordinates the WWP2-dependent ubiquitination of ALIX after PAR1 activation, which appears to serve as a critical regulatory function in the lysosomal sorting of PAR1 (Figure 9D).

DISCUSSION

We previously discovered a novel lysosomal sorting pathway for GPCRs mediated by the adaptor protein ALIX that bypasses ubiquitin-binding ESCRTs and receptor ubiquitination (Dores *et al.*, 2012a). The ALIX lysosomal pathway illustrates the diversity of intracellular sorting mechanisms that regulate signaling receptors like GPCRs and other transmembrane proteins. However, little is known about the ALIX lysosomal pathway or how GPCR sorting through this pathway is regulated. In this study, we describe a new mechanism for the regulation of ALIX-dependent GPCR lysosomal sorting that requires the α-arrestin ARRDC3. We show that ARRDC3 mediates the ubiquitination of ALIX through the recruitment of the E3 ubiquitin ligase WWP2. These findings reveal a novel role for ARRDC3-mediated ubiquitination of ALIX in the lysosomal sorting of the GPCR PAR1.

The mammalian α-arrestins have emerged as adaptor proteins that may regulate endosomal sorting of GPCRs; however, their exact role remains controversial. Unlike β-arrestins, the α-arrestins (with the exception of ARRDC5) contain PPXY motifs that are bound by the WW-domains of NEDD4-family E3 ubiquitin ligases (Rauch and Martin-Serrano, 2011). Therefore the α-arrestins may function as adaptors for the recruitment of ubiquitination machinery to GPCRs. Initial reports suggested that ARRDC3 facilitates the ubiquitination and degradation of activated β2AR by mediating the recruitment of NEDD4-family E3 ubiquitin ligases (Nabhan *et al.*, 2010). Subsequent studies demonstrated that multiple α-arrestins facilitate the ubiquitination of β2AR and the vasopressin 2 receptor (Shea *et al.*,

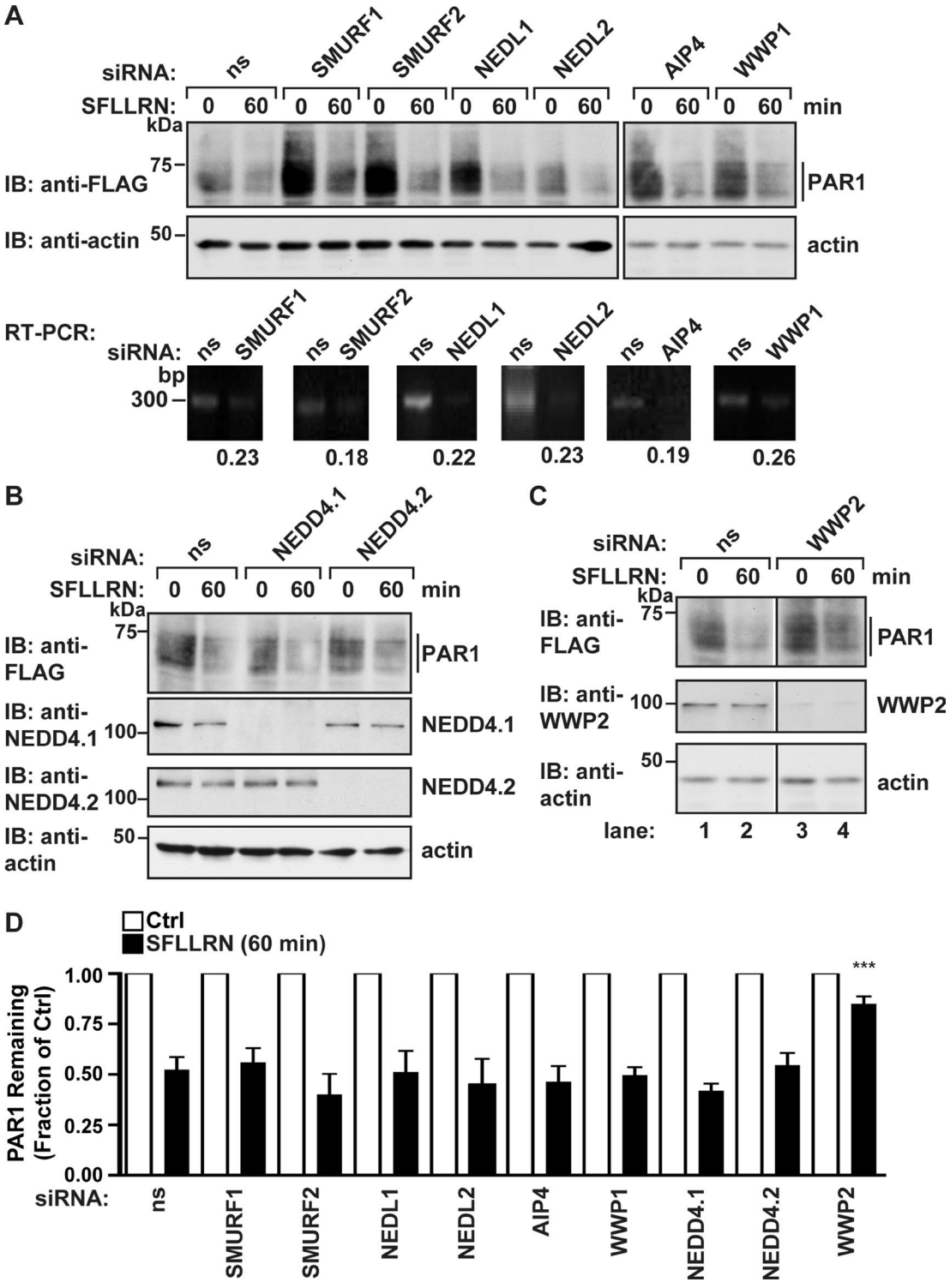

FIGURE 7: WWP2 is required for PAR1 degradation. (A–C) HeLa cells expressing FLAG-PAR1 were transfected with nonspecific (ns) siRNA or siRNAs targeting each of the nine human NEDD4-family HECT E3-ubiquitin ligases and then stimulated with 100 μM SFLLRN. Cell lysates were collected and analyzed by immunoblot. (A) mRNA from HeLa cells expressing FLAG-PAR1 transfected with siRNAs targeting AIP4, WWP1, SMURF1, SMURF2, NEDL1, and NEDL2 was PCR amplified using primers targeting the open reading frame of each ligase. The amount of amplified product was quantified by densitometry, and values represent the fraction of nonspecific control. (D) The extent of PAR1 degradation was measured by densitometry, and the data (mean ± SD, $n = 3$) were analyzed using two-way ANOVA (***$p < 0.001$).

2012). However, these findings were challenged by the discovery that the β-arrestins primarily direct β2AR ubiquitination before lysosomal degradation and that depletion of ARRDC3 does not affect β2AR lysosomal sorting (Han *et al.*, 2012). Instead, α-arrestin–mediated β2AR ubiquitination may regulate nonlysosomal endosomal trafficking that could modulate signaling or recycling. Our findings

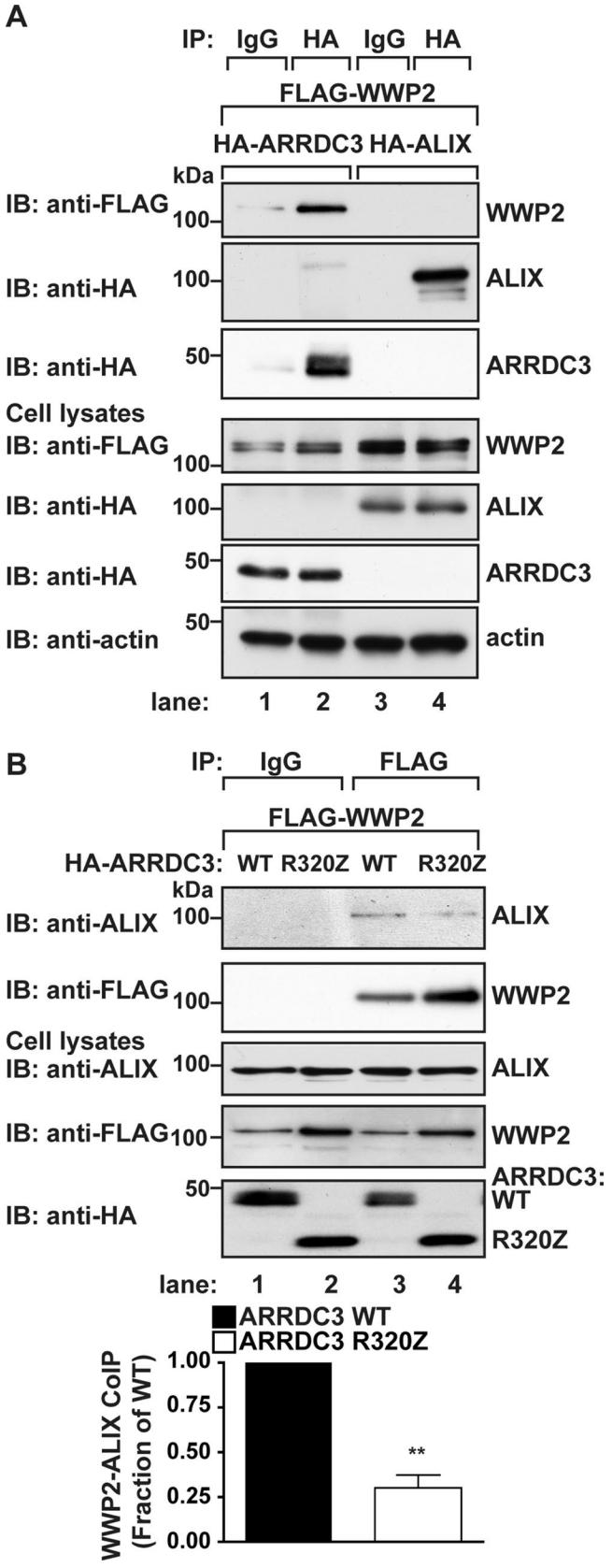

FIGURE 8: ARRDC3 mediates WWP2 interaction with ALIX. (A) COS7 cells were cotransfected with FLAG-WWP2 and either HA-ARRDC3 or HA-ALIX. Cell lysates were immunoprecipitated with anti-HA or IgG control antibodies, and precipitates were analyzed by immunoblot with anti-FLAG antibodies. (B) COS7 cells were cotransfected with FLAG-WWP2 and either HA-ARRDC3 WT or HA-ARRDC3 R320Z. Cell lysates were immunoprecipitated with anti-FLAG antibody, and precipitates were analyzed by immunoblot with anti-ALIX antibodies. Endogenous ALIX coprecipitation was quantified by densitometry, and the data (mean ± SD, $n = 3$) were analyzed using Student's t test (**$p < 0.01$).

demonstrate that ARRDC3 is not required for the degradation of PAR2, a ubiquitinated GPCR that is sorted to the lysosome via the canonical ESCRT pathway (Hasdemir *et al.*, 2007), suggesting that ARRDC3 is not required for the lysosomal sorting of ubiquitinated GPCRs. Our results support a mechanism by which ARRDC3 regulates GPCR lysosomal sorting by mediating the ubiquitination of the adaptor protein ALIX and not the receptor.

Recent studies have uncovered the role of ubiquitination in the regulation of adaptor proteins that facilitate the multivesicular endosomal sorting of mammalian GPCRs. The ESCRT-0 subunit HRS is a critical adaptor protein that binds to ubiquitinated GPCRs such as CXCR4, a GPCR for the chemokine SDF-1 (Marchese *et al.*, 2003). HRS becomes ubiquitinated after CXCR4 activation, a process that is required for sorting of CXCR4 into multivesicular endosomes (Malik and Marchese, 2010; Sierra *et al.*, 2010). Of interest, β–arrestin-1 recruits the NEDD4-family E3 ubiquitin ligase AIP4 to late endosomes (Bhandari *et al.*, 2007), facilitating the ubiquitination of HRS (Malik and Marchese, 2010). HRS ubiquitination stabilizes interaction with the ESCRT-I complex subunit TSG101 (Malik and Marchese, 2010). These studies represent the first evidence that β-arrestin–dependent ubiquitination of adaptor proteins regulates membrane trafficking of GPCRs.

Here we report a novel role for the α-arrestin ARRDC3 in facilitating ubiquitination of ALIX during activated GPCR lysosomal sorting. We demonstrate that ARRDC3 is essential for PAR1 lysosomal sorting and that depletion of endogenous ARRDC3 inhibits ALIX binding to PAR1 and to the ESCRT-III subunit CHMP4B. We also found that ARRDC3 is required for ALIX ubiquitination in response to activation of PAR1. We observed that the pattern of ALIX ubiquitination varies slightly but always includes monoubiquitinated and polyubiquitinated forms that are sensitive to ARRDC3 depletion. Future studies will focus on the function of ALIX monoubiquitination and polyubiquitination in the regulation of ALIX. Ubiquitination of ALIX has also been observed during the budding of viruses from the plasma membrane (Sette *et al.*, 2010), a process that requires ESCRTs and ALIX to package viral particles into membrane buds. ARRDC3 facilitates ALIX ubiquitination during viral budding, and ALIX ubiquitination is required for viral particle release (Rauch and Martin-Serrano, 2011). These findings suggest that ubiquitination regulates ALIX function during the packaging of cargo at the plasma membrane and at the late endosome.

Ubiquitin may regulate ALIX by facilitating ALIX dimerization. ALIX harbors a highly conserved ubiquitin-binding domain (Keren-Kaplan *et al.*, 2013; Pashkova *et al.*, 2013) that is required for ALIX dimerization in vitro (Keren-Kaplan *et al.*, 2013). ALIX dimerization mediates interaction with ESCRT-III filaments that form on membranes during viral budding (Pires *et al.*, 2009), and disruption of ALIX dimerization inhibits the release of HIV (Pires *et al.*, 2009; Bissig *et al.*, 2013). ALIX dimers colocalize with internalized PAR1 and ARRDC3 (Figure 1C), and our findings suggest that ALIX ubiquitination is required for the lysosomal sorting of PAR1. Future studies will interrogate the function of ARRDC3 and WWP2 in regulating ALIX dimerization during GPCR sorting and will investigate the function of the ALIX ubiquitin-binding domain in the trafficking of GPCRs.

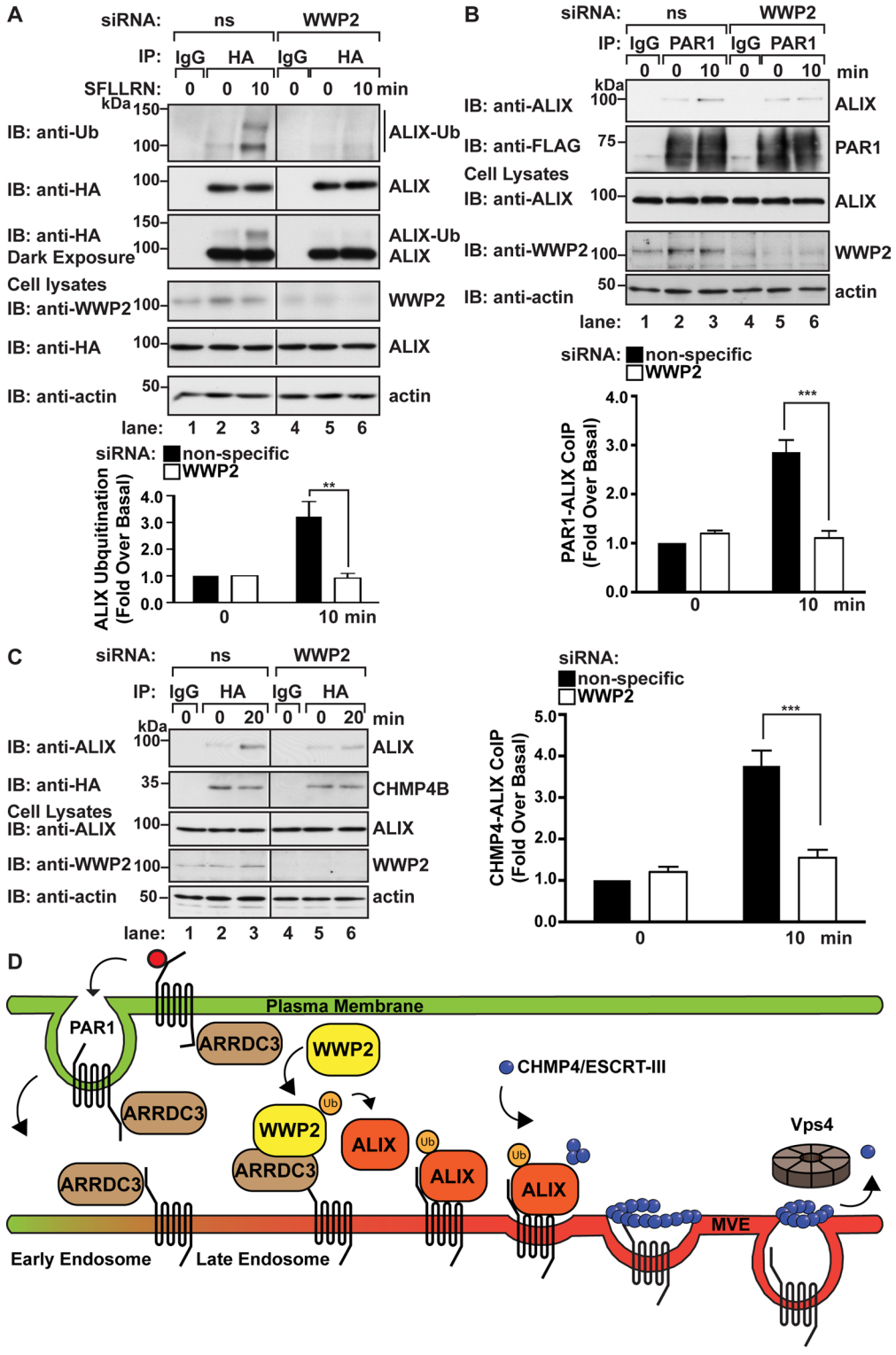

FIGURE 9: WWP2 mediates ALIX ubiquitination and binding to PAR1 and CHMP4B. (A) PAR1 HeLa cells were transfected with HA-ALIX and either nonspecific (ns) or WWP2 siRNAs and then stimulated for the indicated times with 100 μM SFLLRN. Cell lysates were immunoprecipitated with anti-HA antibody. ALIX ubiquitination was quantified by densitometry, and the data (mean ± SD, $n = 3$) were analyzed using two-way ANOVA (**$p < 0.01$). (B) HeLa cells expressing FLAG-PAR1 were cotransfected with either nonspecific (ns) or WWP2 siRNAs and then stimulated with 100 μM SFLLRN. Cell lysates were immunoprecipitated with anti-FLAG antibody. ALIX coprecipitation was quantified by densitometry, and the data (mean ± SD, $n = 3$) were analyzed using two-way ANOVA (***$p < 0.001$). (C) HeLa cells expressing FLAG-PAR1 were cotransfected with HA-CHMP4B and either nonspecific (ns) or WWP2 siRNAs and then stimulated for the indicated times with 100 μM SFLLRN. Cell lysates were immunoprecipitated with anti-HA antibody. ALIX coprecipitation was quantified by densitometry, and the data (mean ± SD, $n = 3$) were analyzed using two-way ANOVA (***$p < 0.001$). (D) Model of ARRDC3-mediated ALIX ubiquitination and PAR1 sorting at the MVE.

ARRDC3 mediates the ubiquitination of ALIX through the recruitment of NEDD4-family E3 ubiquitin ligases. Because ARRDC3 can interact with multiple NEDD4-family E3 ligases (Rauch and Martin-Serrano, 2011; Han *et al.*, 2012; Shea *et al.*, 2012), we screened all nine human NEDD4-family E3 ligases for their function in PAR1 degradation. Although depletion of SMURF1 and SMURF2 increased the basal levels of surface PAR1, it did not effect agonist-induced receptor degradation. However, depletion of WWP2 alone was sufficient to block agonist-induced PAR1 degradation. Of importance, WWP2 is required for ALIX ubiquitination in response to PAR1 stimulation. Although some reports suggested that ALIX can interact directly with NEDD4.1 (Sette *et al.*, 2010), we observed that ARRDC3 facilitates the interaction between ALIX and WWP2. Similarly to ARRDC3, WWP2 depletion also blocks ALIX binding to PAR1 and CHMP4B. In contrast, during viral budding, ARRDC3 recruits NEDD4.1 to ubiquitinate ALIX and mediates the recruitment of ESCRTs (Rauch and Martin-Serrano, 2011). Thus ARRDC3 appears to mediate ALIX ubiquitination through multiple E3 ubiquitin ligases in a context-dependent manner. In addition, ARRDC3 WT overexpression appears to reduce the expression of WWP2 in comparison to cells expressing a mutant of ARRDC3 lacking its C-terminus. However, overexpression of ARRDC3 WT does not appear to affect the expression of other E3 ligases, such as NEDD4.1 (Nabhan *et al.*, 2010). It will be important to determine the factors that may influence ARRDC3 recruitment and regulation of different E3 ubiquitin ligases in order to facilitate ALIX ubiquitination.

In summary, our study has revealed a novel mechanism for the regulation of ALIX-dependent GPCR lysosomal sorting by the α-arrestin ARRDC3. Our results support a model in which ARRDC3 recruits the NEDD4-family E3 ubiquitin ligase WWP2 to PAR1 at late endosomes to ubiquitinate ALIX, facilitating the sorting of PAR1 into intraluminal vesicles of MVE's (Figure 9D). However, the mechanisms that regulate ARRDC3 and WWP2 after activation of PAR1 signaling are unclear. Recent work demonstrated that the NEDD4-family E3 ligase AIP4 is itself ubiquitinated and regulated by a RING-E3 ligase, Deltex3L in response to CXCR4 activation (Holleman and Marchese, 2014). However, the signaling effectors that regulate Deltex3L activity are not known. It is unclear whether phosphorylation or ubiquitination regulates ARRDC3 and WWP2 activity after PAR1 stimulation. Thus further studies are required to link GPCR signaling to ARRDC3- and WWP2-mediated ALIX ubiquitination at late endosomes.

MATERIALS AND METHODS

Antibodies and reagents

PAR1 peptide agonist (SFLLRN) and PAR2 peptide agonist (SLIGKV) were synthesized and purified by reverse-phase, high-pressure liquid chromatography at the Tufts University Core Facility (Boston, MA). Epidermal growth factor was purchased from Sigma-Aldrich (St. Louis, MO). Polyclonal anti-FLAG and anti-HA antibodies were purchased from Rockland Immunochemicals (Pottstown, PA). Anti-EEA1 antibody was obtained from BD Biosciences (East Rutherford, NJ). Monoclonal anti-PAR1 WEDE antibody was purchased from Beckman Coulter (Brea, CA). Polyclonal anti-ARRDC3, monoclonal anti-ALIX, and monoclonal anti-Ub (P4D1) antibodies were purchased from Santa Cruz Biotechnology (Santa Cruz, CA). Anti-EGFR antibody was obtained from Cell Signaling Technologies (Boston, MA). Monoclonal anti-HA antibody was purchased from Covance (San Diego, CA). Horseradish peroxidase–conjugated goat anti-rabbit and goat anti-mouse antibodies were purchased from Bio-Rad Laboratories (Hercules, CA). Alexa Fluor 488, 594, and 647 secondary antibodies were purchased from Invitrogen (Carlsbad, CA).

Plasmids and cell lines

The full-length human N-terminal, FLAG-tagged PAR1 WT, FLAG-PAR1 0K, and FLAG-PAR2 WT cDNAs cloned into the mammalian expression vector pBJ were described previously (Trejo *et al.*, 2000; Wolfe *et al.*, 2007; Ricks and Trejo, 2009). The PAR1-YFP cDNA and ARRDC3-RLuc cDNA construct were cloned into the pcDNA3.1 vector for this study. The HA-ARRDC3 WT cDNA cloned into the pcDNA3.1 vector was provided by Q. Lu (Harvard University, Cambridge, MA). The HA-ALIX WT cDNA cloned into the pcDNA3.1 vector was provided by J. Martin-Serrano (King's College, London, United Kingdom). The GFP-Rab5 WT and GFP-Rab5 Q79L cDNAs were provided by A. Marchese (Loyola University, Maywood, IL). The split-YFP ALIX-ΔPRD plasmids were provided by J. Gruenberg (University of Geneva, Geneva, Switzerland). HeLa cells stably expressing FLAG-PAR1, FLAG-PAR1 0K, or FLAG-PAR2 cloned into pBJ vectors were generated by cotransfection with a plasmid encoding a hygromycin-resistance gene, selected in 250 μg/ml hygromycin, and screened by cell surface ELISA (Trejo *et al.*, 2000). COS-7 cells were transiently transfected with PAR1-YFP and/or ARRDC3-Rluc plasmids for BRET analysis. COS-7 cells were cotransfected with FLAG-WWP2 and either HA-ARRDC3 or HA-ALIX for coimmunoprecipitation studies.

siRNA and cDNA transfections

HeLa cells were transfected with plasmid DNA using 1 mg/ml polyethylenimine (PEI) at a 6:1 ratio (6 μl PEI:1 μg plasmid). siRNA transfection was performed using Oligofectamine (Invitrogen) per manufacturer's instructions. All single siRNAs were purchased from Qiagen or Invitrogen: nonspecific, 5′-GGCTACGTCCAGGAGCGCACC-3′; ALIX #1, 5′-AAGTACCTCAGTCTATATTGA-3′; ALIX #3, 5′-AATCGAGACGCTCCTGAGATA-3′; ARRDC3, 5′-AAGGGAAAATGAAGGAAGTAA-3′; NEDD4.1, 5′-CCGGAGAATTATGGGTGTCAA-3′; NEDD4.2, 5′-AAGATCATAACACAAAGACTA-3′; WWP1, 5′-AAGAAGTCATCTGTAACTAAA-3′; WWP2, 5′-TAGACACGTCCGTTGGGCAGCTCTC-3′; SMURF1, 5′-GCATCGAAGTGTCCAGAGAAG-3′; SMURF2, 5′-CCGGATCTTCACAACAGTTTA-3′; NEDL1, 5′-AAGATGAGGTCTTGTCCGAAA-3′; and NEDL2, 5′-AAGTGGGTACCTCCAGTTTAA-3′. SMARTpool siRNAs were purchased from Dharmacon: AIP4, 5′-GGTGACAAAGAGCCAACAGAG-3′.

Reverse transcriptase-PCR

The first-strand cDNA was generated from mRNA extracted from either HeLa using SuperScript II Reverse Transcriptase (Invitrogen) following the manufacturer's instructions. The reverse transcriptase enzyme was omitted from the cDNA synthesis reaction in the control samples. The first-strand cDNA was amplified via PCR using primer pairs specific for SMURF1, forward, 5′-GCCTGTACTGGACCACACCT-3′, and reverse, 5′-TGAGCTCATTGAACCCCTTC-3′; SMURF2, forward, 5′-ATGGTTCTGGAAAGCTGTGG-3′, and reverse, 5′-TTCGATTGAAGCAAGTGTGG-3′; NEDL1, forward, 5′-GTTTTGTGTCCTTGCCCACT-3′, and reverse, 5′-GAATTGCAGCTGTCCACTCA-3′; NEDL2, forward, 5′-GACCGAGTCTCTCGATCAGG-3′, and reverse, 5′-AAGAGAGGAGCACCGTGTGT-3′; and AIP4, forward, 5′-GTTGGGAGCAGAGAGTGGAC-3′, and reverse, 5′-TCATAGTTCCGGACGGATTC-3′. The PCR amplification products were resolved by 1.8% (wt/vol) agarose gel electrophoresis and visualized by ethidium bromide staining.

Bioluminescence resonance energy transfer

COS-7 cells were transfected with 0.1 μg of ARRDC3-Rluc and a range (0–1.0 μg) of PAR1-YFP for 48 h, detached with Cellstripper

(Mediatech, Manassas, VA), washed three times with phosphate-buffered saline (PBS), and resuspended in PBS containing 0.5 mM $MgCl_2$ and 0.1% glucose at a density of 5×10^5 cells/ml. Cells (90 µl) were added to a 96-well microplate in triplicate, and 10 µl of coelenterazine h substrate was added (final concentration, 5 µM). After an 8-min delay, signals were determined with a TriStar LB 941 plate reader (Berthold Biotechnologies) using two filter settings at 480 and 535 nm and MicroWIN 2000 software (Berthold Technologies, Oak Ridge, TN). The YFP signal was determined by exciting at 485 nm and detecting at 535 nm. Total luminescence was measured by integrating the signal for 1 s/well without filter selection. Net BRET was calculated as previously described (Lin and Trejo, 2013). Data from three independent experiments were pooled and fitted with nonlinear regression using Prism software (GraphPad, San Diego, CA).

PAR1 degradation assays

HeLa cells stably transfected with FLAG-PAR1 WT, FLAG-PAR1 0K, or FLAG-PAR2 WT were plated in 12-well plates (0.75×10^5 cells/well) and grown overnight at 37°C. Cells were transfected with siRNA. For siRNA knockdown-rescue experiments, cells were first transfected with plasmids and then siRNA after an overnight incubation. After 48 h, cells were washed and then incubated with or without 100 µM SFLLRN (PAR1) or 100 µM SLIGKV (PAR2) at 37°C for the indicated times. Cells were then placed on ice, washed with PBS, and lysed in Triton X-100 lysis buffer (50 mM Tris-HCl, pH 7.4, 100 mM NaCl, 5 mM EDTA, 50 mM NaF, 10 mM sodium pyrophosphate, and 1% [vol/vol] Triton X-100) supplemented with protease inhibitors. Cell lysates were collected and sonicated for 10 s at 10% amplitude (Branson Model 450 sonifier), and protein concentration was normalized after quantification by bicinchoninic acid assay (Thermo Fisher Scientific, Waltham, MA). Equivalent amounts of lysates were used for analysis by immunoblotting.

Immunoprecipitation

HeLa cells stably expressing FLAG-PAR1 WT were grown in six-well plates (2.0×10^5 cells/well) overnight at 37°C and then transfected with either HA-ALIX or HA-CHMP4B plasmid. Cells were incubated for 48 h, washed, and then stimulated for the indicated times with 100 µM SFLLRN. For coimmunoprecipitations: Cells were washed and then lysed with NP-40 buffer (0.5% [vol/vol] NP40, 20 mM Tris-HCl, pH 7.4, 150 mM NaCl) supplemented with protease inhibitors and 3 mg/ml N-ethylmaleimide (NEM). For ubiquitination assays, cells were washed and then lysed with RIPA buffer (5 mM EDTA, 50 mM Tris-HCl, pH 8.0, 0.5% [wt/vol] Na deoxycholate, 1% [vol/vol] NP-40, 0.1% [wt/vol], 1% SDS) supplemented with protease inhibitors and 3 mg/ml NEM or 10 µM PR-619 (Boston Biochem, Boston, MA). Lysates were sonicated for 10 s at 10% amplitude and then clarified by centrifugation at 14,000 rpm for 30 min at 4°C. Clarified lysates were incubated with protein A–Sepharose beads (GE Healthcare, Pittsburgh, PA) and the indicated antibodies overnight at 4°C. Beads were washed and resuspended in 2× Laemmli sample buffer. Immunoprecipitates were resolved on 6% SDS–PAGE gels to separate higher–molecular weight ubiquitinated ALIX from unmodified ALIX and then transferred onto polyvinylidene fluoride and immunoblotted using anti-ubiquitin antibody.

Immunofluorescence microscopy

HeLa cells stably expressing FLAG-PAR1 WT were plated on coverslips in 12-well plates (0.75×10^5 cells/well) and incubated overnight at 37°C. Cells were transfected with the indicated plasmids and then incubated for 48 h. For the indicated experiments, cells were pretreated with 2 mM leupeptin for 1 h at 37°C to inhibit lysosomal degradation. Cells were washed and then labeled with anti-FLAG antibody at 4°C for 1 h to track the surface cohort of receptor. Cells were washed and then stimulated with 100 µM SFLLRN for the indicated times. Cells were fixed in 4% paraformaldehyde, permeabilized in 100% methanol, and treated with the indicated primary and secondary antibodies. Coverslips were mounted using Fluorsave reagent (EMD Biochemical, Billerica, MA). Images were acquired with a spinning-disk confocal system (Olympus, Waltham, MA) configured with a microscope (IX81; Olympus) fitted with a PlanApo 60× oil objective (1.4 numerical aperture; Olympus) and a digital camera (ORCA-ER; Hamamatsu Photonics, San Diego, CA). Fluorescence images of 0.28-µm-thick *XY*-sections were acquired at room temperature using SlideBook 5.0 software (Intelligent Imaging Innovations, Denver, CO). Values of Pearson's *r* for quantifying colocalization were calculated from at least six independent cells from multiple experiments using SlideBook 5.0.

Statistics

Data were analyzed using Prism software (version 4.0; GraphPad Software). Statistical analysis was determined, as indicated, by performing either Student's *t* test or two-way analysis of variance (ANOVA).

ACKNOWLEDGMENTS

We thank members of the Trejo laboratory for comments and suggestions and Thomas Smith for technical assistance. This work was supported by National Institutes of Health/National Institute of General Medical Sciences Grant R01 GM090689 (to J.T.). M.R.D. is a San Diego IRACDA Fellow supported by National Institutes of Health Grant K12 GM06852.

REFERENCES

Alvarez CE (2008). On the origins of arrestin and rhodopsin. BMC Evol Biol 8, 222.

Bhandari D, Trejo J, Benovic JL, Marchese A (2007). Arrestin-2 interacts with the ubiquitin-protein isopeptide ligase atrophin-interacting protein 4 and mediates endosomal sorting of the chemokine receptor CXCR4. J Biol Chem 282, 36971–36979.

Bissig C, Lenoir M, Velluz M-C, Kufareva I, Abagyan R, Overduin M, Gruenberg J (2013). Viral infection controlled by a calcium-dependent lipid-binding module in ALIX. Dev Cell 25, 364–373.

Chen B, Dores MR, Grimsey N, Canto I, Barker BL, Trejo J (2011). Adaptor protein complex-2 (AP-2) and epsin-1 mediate protease-activated receptor-1 internalization via phosphorylation- and ubiquitination-dependent sorting signals. J Biol Chem 286, 40760–40770.

Dores MR, Chen B, Lin H, Soh UJK, Paing MM, Montagne WA, Meerloo T, Trejo J (2012a). ALIX binds a YPX3L motif of the GPCR PAR1 and mediates ubiquitin-independent ESCRT-III/MVB sorting. J Cell Biol 197, 407–419.

Dores MR, Paing MM, Lin H, Montagne WA, Marchese A, Trejo J (2012b). AP-3 regulates PAR1 ubiquitin-independent MVB/lysosomal sorting via an ALIX-mediated pathway. Mol Biol Cell 23, 3612–3623.

Duan L, Miura Y, Dimri M, Majumder B, Dodge IL, Lakku Reddi A, Ghosh AK, Fernandes N, Zhou P, *et al.* (2003). Cbl-mediated ubiquitinylation is required for lysosomal sorting of EGF receptor but is dispensable for endocytosis. J Biol Chem 278, 28950–28960.

Gullapalli A, Wolfe BL, Griffin CT, Magnuson T, Trejo J (2006). An essential role for SNX1 in lysosomal sorting of protease-activated receptor-1: evidence for retromer-, Hrs-, and Tsg101-independent functions of sorting nexins. Mol Biol Cell 17, 1228–1238.

Han SO, Kommaddi RP, Shenoy SK (2012). Distinct roles for beta-arrestin2 and arrestin-domain-containing proteins in beta(2) adrenergic receptor trafficking. EMBO Rep 14, 164–171.

Hasdemir B, Bunnett NW, Cottrell GS (2007). Hepatocyte growth factor-regulated tyrosine kinase substrate (HRS) mediates post-endocytic trafficking of protease-activated receptor 2 and calcitonin receptor-like receptor. J Biol Chem 282, 29646–29657.

Hasdemir B, Murphy JE, Cottrell GS, Bunnett NW (2009). Endosomal deubiquitinating enzymes control ubiquitination and down-regulation of protease-activated receptor 2. J Biol Chem 284, 28453–28466.
Henry AG, White IJ, Marsh M, von Zastrow M, Hislop JN (2011). The role of ubiquitination in lysosomal trafficking of delta-opioid receptors. Traffic 12, 170–184.
Holleman J, Marchese A (2014). The ubiquitin ligase deltex-3l regulates endosomal sorting of the G protein-coupled receptor CXCR4. Mol Biol Cell 25, 1892–1904.
Keren-Kaplan T, Attali I, Estrin M, Kuo LS, Farkash E, Jerabek-Willemsen M, Blutraich N, Artzi S, Peri A, Freed EO, *et al*. (2013). Structure-based in silico identification of ubiquitin-binding domains provides insights into the ALIX-V:ubiquitin complex and retrovirus budding. EMBO J 32, 538–551.
Lin H, Trejo J (2013). Transactivation of the PAR1-PAR2 heterodimer by thrombin elicits β-arrestin-mediated endosomal signaling. J Biol Chem 288, 11203–11215.
Malik R, Marchese A (2010). Arrestin-2 interacts with the endosomal sorting complex required for transport machinery to modulate endosomal sorting of CXCR4. Mol Biol Cell 21, 2529–2541.
Marchese A, Paing MM, Temple BRS, Trejo J (2008). G protein-coupled receptor sorting to endosomes and lysosomes. Annu Rev Pharmacol Toxicol 48, 601–629.
Marchese A, Raiborg C, Santini F, Keen JH, Stenmark H, Benovic JL (2003). The E3 ubiquitin ligase AIP4 mediates ubiquitination and sorting of the G protein-coupled receptor CXCR4. Dev Cell 5, 709–722.
Marchese A, Trejo J (2012). Ubiquitin-dependent regulation of G protein-coupled receptor trafficking and signaling. Cell Signal 25, 707–716.
Mason JS, Bortolato A, Congreve M, Marshall FH (2012). New insights from structural biology into the druggability of G protein-coupled receptors. Trends Pharmacol Sci 33, 249–260.
McCullough J, Fisher RD, Whitby FG, Sundquist WI, Hill CP (2008). ALIX-CHMP4 interactions in the human ESCRT pathway. Proc Natl Acad Sci USA 105, 7687–7691.
Nabhan JF, Pan H, Lu Q (2010). Arrestin domain-containing protein 3 recruits the NEDD4 E3 ligase to mediate ubiquitination of the beta2-adrenergic receptor. EMBO Rep 11, 605–611.
O'Hayre M, Degese MS, Gutkind JS (2014). Novel insights into G protein and G protein-coupled receptor signaling in cancer. Curr Opin Cell Biol 27, 126–135.
O'Keeffe MB, Reid HM, Kinsella BT (2008). Agonist-dependent internalization and trafficking of the human prostacyclin receptor: a direct role for Rab5a GTPase. Biochim Biophys Acta 1783, 1914–1928.
Pashkova N, Gakhar L, Winistorfer SC, Sunshine AB, Rich M, Dunham MJ, Yu L, Piper RC (2013). The yeast Alix homolog Bro1 functions as a ubiquitin receptor for protein sorting into multivesicular endosomes. Dev Cell 25, 520–533.
Pires R, Hartlieb B, Signor L, Schoehn G, Lata S, Roessle M, Moriscot C, Popov S, Hinz A, Jamin M, *et al*. (2009). A crescent-shaped ALIX dimer targets ESCRT-III CHMP4 filaments. Structure 17, 843–856.
Rauch S, Martin-Serrano J (2011). Multiple interactions between the ESCRT machinery and arrestin-related proteins: implications for PPXY-dependent budding. J Virol 85, 3546–3556.
Ricks TK, Trejo J (2009). Phosphorylation of protease-activated receptor-2 differentially regulates desensitization and internalization. J Biol Chem 284, 34444–34457.
Sette P, Jadwin JA, Dussupt V, Bello NF, Bouamr F (2010). The ESCRT-associated protein Alix recruits the ubiquitin ligase Nedd4-1 to facilitate HIV-1 release through the LYPXnL L domain motif. J Virol 84, 8181–8192.
Sette P, Nagashima K, Piper RC, Bouamr F (2013). Ubiquitin conjugation to Gag is essential for ESCRT-mediated HIV-1 budding. Retrovirology 10, 79.
Shea FF, Rowell JL, Li Y, Chang TH, Alvarez CE (2012). Mammalian alpha arrestins link activated seven transmembrane receptors to nedd4 family e3 ubiquitin ligases and interact with Beta arrestins. PLoS One 7, e50557.
Shenoy SK, Xiao K, Venkataramanan V, Snyder PM, Freedman NJ, Weissman AM (2008). Nedd4 mediates agonist-dependent ubiquitination, lysosomal targeting, and degradation of the beta2-adrenergic receptor. J Biol Chem 283, 22166–22176.
Sierra MI, Wright MH, Nash PD (2010). AMSH interacts with ESCRT-0 to regulate the stability and trafficking of CXCR4. J Biol Chem 285, 13990–14004.
Soh UJK, Trejo J (2011). Activated protein C promotes protease-activated receptor-1 cytoprotective signaling through β-arrestin and dishevelled-2 scaffolds. Proc Natl Acad Sci USA 108, E1372–E1380.
Stenmark H, Parton RG, Steele-Mortimer O, Lutcke A, Gruenberg J, Zerial M (1994). Inhibition of rab5 GTPase activity stimulates membrane fusion in endocytosis. EMBO J 13, 1287–1296.
Trejo J, Altschuler Y, Fu H-W, Mostov KE, Coughlin SR (2000). Protease-activated receptor-1 down-regulation. J Biol Chem 275, 31255–31265.
Vu T-KH, Hung DT, Wheaton VI, Coughlin SR (1991). Molecular cloning of a functional thrombin receptor reveals a novel proteolytic mechanism of receptor activation. Cell 64, 1057–1068.
Wolfe BL, Marchese A, Trejo J (2007). Ubiquitination differentially regulates clathrin-dependent internalization of protease-activated receptor-1. J Cell Biol 177, 905–916.